

DESIGN EVALUATIONS OF DOUBLE ROTOR SWITCHED RELUCTANCE MACHINE

C.V. ARAVIND^{1,*}, AIMAN SAJA¹, VIJAYSHANKAR²

¹School of Engineering, Taylor's University, Taylor's Lakeside Campus,
No. 1 Jalan Taylor's, 47500, Subang Jaya, Selangor DE, Malaysia

²Department of Electrical and Electronics Engineering,
Sona College of Technology, Salem

*Corresponding Author: aravindcv@ieee.org

Abstract

The absence of magnets makes the reluctance machine typical for low cogging operations with the torque depending on the stator rotor interaction area. The air gap between stator pole and rotor pole gives a huge effect on the reluctance variation. The primitive double rotor switched reluctance machine lags to improvise the effect of the ripple value though the torque density is higher compared to conventional machines. An optimised circular hole position and dimensioned in the stator pole of lowers the torque ripple and reduce the acoustic noise as presented in this paper. A comparative evaluation of the conventional double rotor machine with this improved structure is done through numerical design and evaluations for the same sizing. It is found that the motor constant square density. It is found that the double rotor switched reluctance machine is improved by 140% to conventional machine.

Keywords: double rotor machine, reluctance machine, electromagnetic analysis, FEA

1. Introduction

Switched reluctance machine has high operational efficiency, large torque to inertia ratio, cheap and simple construction which clearly shows that this machine is chosen over other conventional machine for various applications variable speed applications [1, 2].

Nowadays, the switched reluctance machine has very high demand in many application due to expensive permanent magnet. Most people are making a research on increase the average torque density of switched reluctance machine over wide speed range of the operating system [3, 4]. Besides that, there are other different approaches that could optimized the switched reluctance machine that could give a huge benefit to the industry and society as well. Switched reluctance machine properties can be improved by ripple torque reduction [5], machine design optimization [6, 7] and current control [8].

An improved novel switched reluctance machine design can be produced by making the previous switched reluctance machine design based on its development and improvement as a guideline which presented in [9, 10]. The previous developed switched reluctance machine design in [11] is assessed. From the assessment made, the torque density production in normal switched reluctance machine relies on distance of air gap between stator and rotor. The torque density production is inversely proportional to the total length of air-gap. Thus, the dual air-gap magnetic circuit is introduced at the double rotor switched reluctance machine design [12]. Since the total length air gap remains the same, the length for each air-gap is reduced and the torque density generation is increased. Conversely, the volume of the double rotor switched reluctance machine much bigger and the average torque density is lower compared to normal switched reluctance machine. Although dual air-gap magnetic circuit has little disadvantages, it offers some improvements in other features for switched reluctance machine, thus, gives a huge opportunity for used in industrial application. The previous novel switched reluctance machine design which has a circular hole in the stator pole is evaluated and presented in [13]. It has been identified the torque ripple is lower compared to conventional switched reluctance machine. In this paper, a dual air-gap with circular-hole magnetic circuit is proposed. An improved novel double rotor switched reluctance machine design with a better torque density capability and lower torque ripple is introduced. To determine and evaluate the machine performance, the finite element analysis is used and motor constant square density of all the machines are being compared where the size and volume for all machine should be same for experimental purpose.

2. Design Methodology

2.1. Design aspects

The torque production of reluctance machine relies on the electromagnetic force in the air gap flux linkage between stator and rotor. As the torque density of reluctance is directly proportional to the air-gap flux linkage, the double rotor switched reluctance machine which has two air-gaps with the machine structure and the equivalent magnetic circuit is as shown in Fig. 1.

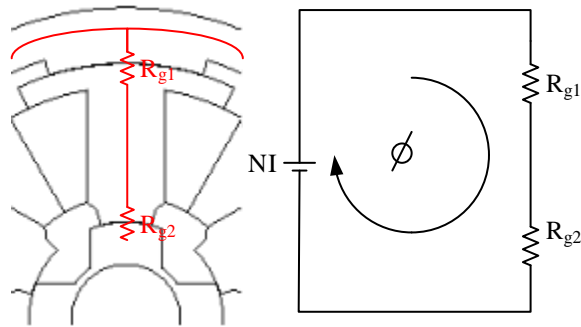


Fig. 1. Double rotor switched reluctance machine.

The total magnetic reluctance for conventional double rotor switched reluctance machine is given in Eq. (1) as,

$$R_t = R_{g1} + R_{g2} \quad (1)$$

where R_t is the total magnetic reluctance, R_{g1} is the first magnetic reluctance at the air-gap and R_{g2} is the second magnetic reluctance at the air-gap. The magnetic flux production for conventional double rotor switched reluctance machine is given in Eq. (2) as,

$$NI = \Phi(R_{g1} + R_{g2}) \quad (2)$$

where N is the number of turns per phase, I is the phase current and Φ is the magnetic flux.

Although, torque density of reluctance machine is improved with dual air-gap magnetic circuit, the ripple torque of reluctance is increased which causes a mechanical vibration and acoustic noise. The circular hole in the tip of stator pole is introduced which can guide the flux linkage direction to the machine rotation. The circular hole is designed instead of square hole or triangle hole due to its-shape. Circular hole occupies large volume compared to other shapes in the same size. Besides that, it does not have edges which can obstruct the flux linkage direction. The dual air-gap with circular hole structure and the equivalent magnetic circuit is as shown in Fig. 2. The presence of circular hole on the stator structure makes the magnetic circuit has two magnetic reluctances in parallel. The total magnetic reluctance for conventional double rotor switched reluctance machine is given in Eqs. (3) and (4),.

$$R_t = R_{g1} + R_{g2} + (R_{ch1} || R_{ch2}) \quad (3)$$

$$R_t = R_{g1} + R_{g2} + \frac{R_{ch1} \times R_{ch2}}{R_{ch1} + R_{ch2}} \quad (4)$$

where R_{ch1} is the first magnetic reluctance at the circular hole and R_{ch2} is the second magnetic reluctance at the circular hole.

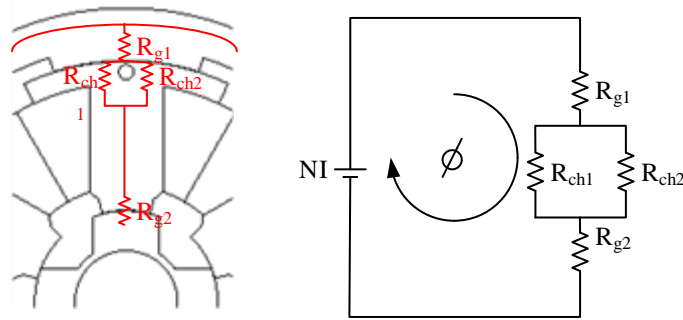


Fig. 2. Improved double rotor switched reluctance machine.

The magnetic flux production for conventional double rotor switched reluctance machine is given in Eq. (5) as:

$$NI = \phi \left(R_{g1} + R_{g2} + \frac{R_{ch1} \times R_{ch2}}{R_{ch1} + R_{ch2}} \right) \quad (5)$$

The structural dimension of the proposed machine is presented in Table 1 and the 3D model design is presented in Fig 3.

Table. 1. Machine specification.

Parameter	Value
Machine diameter	80 mm
Inner air-gap length	0.05 mm
Outer air-gap length	0.05 mm
Outer rotor pole arc	35°
Inner rotor pole arc	42°
Outer stator teeth pole arc	50°
Inner stator teeth pole arc	30°
Circular hole diameter	1 mm
Number of turns per phase	116 turns

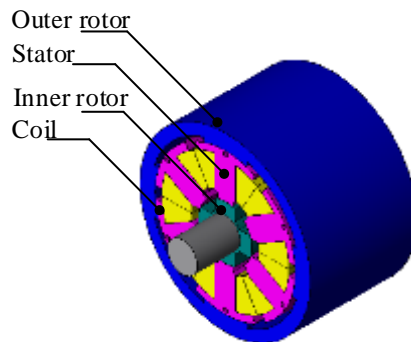


Fig. 3. Improved double rotor switched reluctance machine.

3. Numerical Analysis

3.1. Finite Element Analysis (FEA)

Finite Element Analysis (FEA) tool is used to compute the torque production of the machine. In research based, the finite element analysis is used as a basic analysis material or object in order to identify the applied stress that occurs in the machine design. It is commonly used as an identifier of potential magnetic vector regardless the magnetic circuit complexity as well as non-linear properties of its magnetic material. In this machine design experiment the finite element analysis of the proposed machine is identified based on the numerical tool. The proposed machine magnetic flux characteristics are presented in Fig. 4. The current on coil winding on this simulation is a single phase supply and its value is 7 A. Figure 4(i) illustrates the complete non-overlap flux line. It means the torque is not been generated yet, thus, the long flux line is shown horizontally. There is a quite large number of magnetic flux line on this proposed machine design. Figures 4(ii)-(v) shows the variation behavior of magnetic flux line on the proposed machine design. Figure 4(vi) shows a flux line at the unaligned position. A small increment angle leads to a single step for torque density increment. Figure 5 shows the two dimensional prototype developed using 3-D printing.

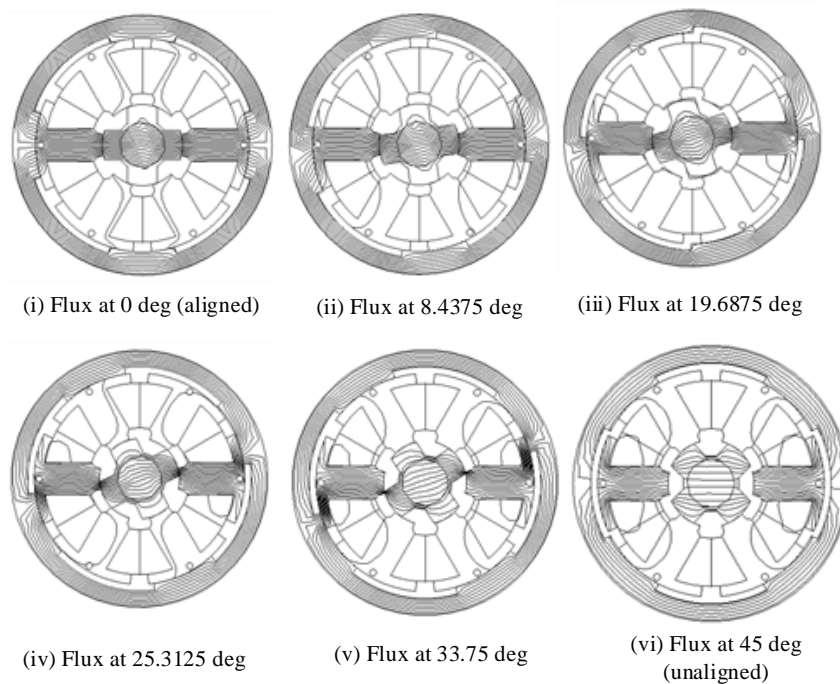


Fig. 4. Proposed double rotor switched reluctance machine circuit.



Fig. 5. Prototype using Printed Circuit Board.

4. Results and Discussions

4.1. Magnetic flux linkage

The magnetic flux linkage for the current value of $7A$ at unaligned and aligned position is shown in Fig. 6. It shows the magnetic flux linkage of proposed machine at unaligned position (a) and aligned position (b). As the proposed machine at unaligned position (a), the maximum value of magnetic flux linkage produces by the machine is $2.8T$ and when the proposed machine at aligned position (b), the maximum value of magnetic flux linkage produces by the machine is $2.4T$. This phenomenon is happened as the machine at aligned position has higher number of flux line go through the machine compared to the machine at unaligned position. As the number of flux line is gradually increases, the magnetic flux linkage is increases as well.

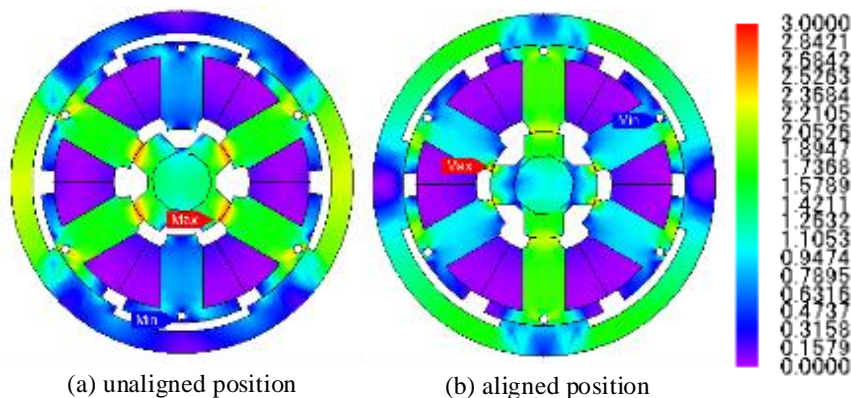


Fig. 6. Magnetic flux linkage.

4.2. Static characteristics

The static characteristics show that the proposed Improved Double Rotor Switched Reluctance Machine (IDRSRM) has higher average torque generation in comparison to conventional Double Rotor Switched Reluctance Machine (DRSRM) as can be seen by the spread out of the characteristics in Fig. 7.

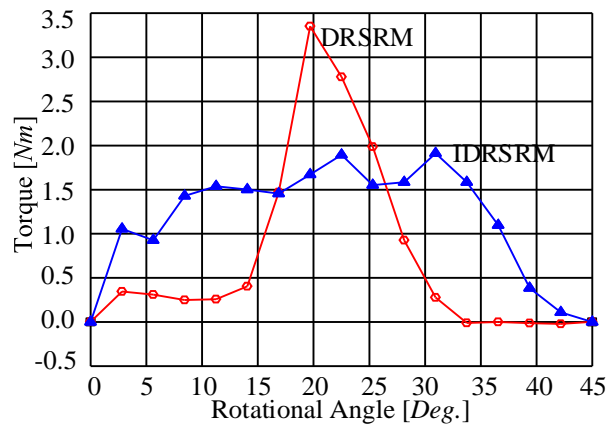


Fig. 7. Static characteristics.

In the static characteristics, the performance of the Improved Double Rotor Switched Reluctance Machine (IDRSRM) is determined for torque, magnetic flux linkage, and machine inductance. All parameters value is analyzed in fixed range of rotors position, from 0° to 45° . The torque waveform of IDRSRM is analyzed in three different phase current values of 3A, 5A, and 7A. The graph of torque against rotational angle for IDRSRM is presented in Fig. 8. The result clearly shows the phase current is directly proportional to the torque density.

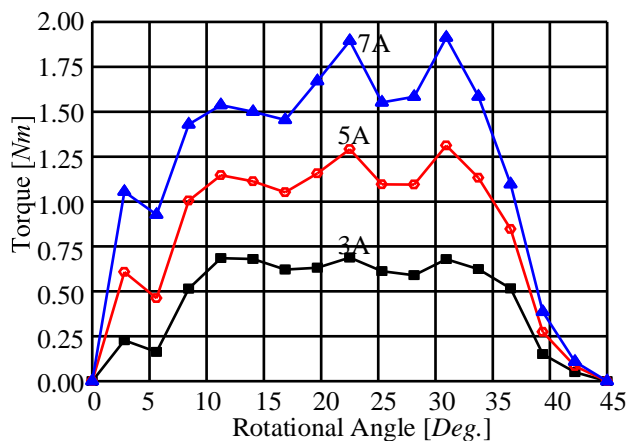


Fig. 8. Static characteristics with different current.

The magnetic flux linkage waveform of the IDRSRM is analyzed for three different phase current values 3A, 5A, and 7A. The graph of magnetic flux against rotational angle for IDRSRM is presented in Fig. 9. The result clearly shows as the phase current increases, the magnetic flux increases as well. The inductance waveform of the IDRSRM is analyzed in three distinct excited current value; 3A, 5A, and 7A. The graph of machine inductance against rotational angle for

IDRSRM is shown in Fig. 10 and it can be inferred that the phase current is directly proportional to the inductance.

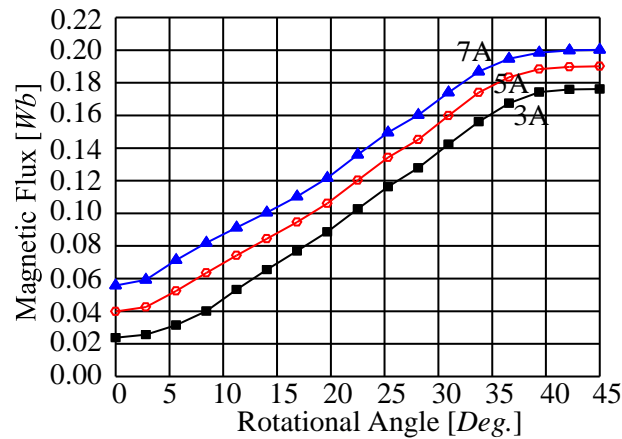


Fig. 9. Magnetic flux characteristics.

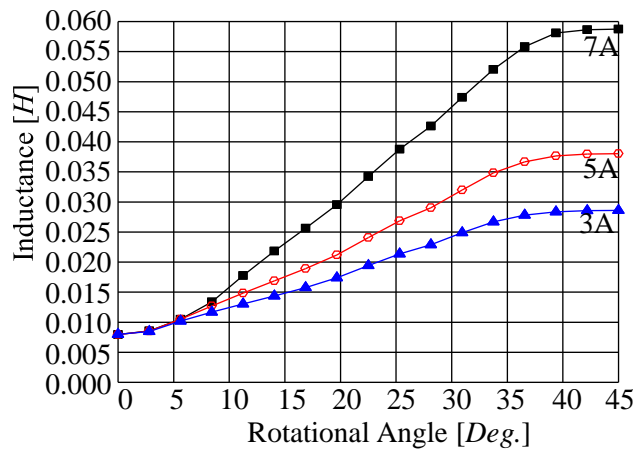


Fig. 10. Inductance characteristics.

4.3. Dynamic characteristics

In the dynamic characteristics, the average torque is determined for speed values of 600 rpm, 1200 rpm, 1800 rpm, 2400 rpm and 3000 rpm. The average torque against operating speed for DRSRM and IDRSRM with a constant step number of 181 and fixed switching angle 5° is shown in Fig. 11. The maximum torque is obtained when the operating speed of the machine is 600 rpm. It is happened because of the machine losses such as heat losses increases along the machine operating speed. The average torque for IDRSRM is not dropped drastically when the operating speed increases unlike DRSRM due to the radial force on the machine. The radial force parameter depends on the machine structure design. The presence of circular-hole structure on the IDRSRM reduces the radial force

which makes the torque of the IDRSRM along the machine operating speed is slightly reduced along the machine operating speed.

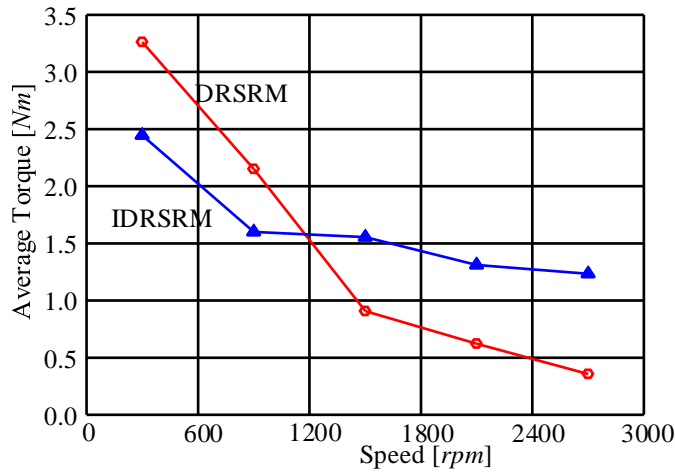


Fig. 11. Dynamic characteristics.

4.4. Comparative Evaluations

For comparison on the level of performance for conventional and proposed structure, the methods of calculation Motor Constant Square Density G is used. The Motor Constant Square Density G is given as in Eq. (6).

$$G = \frac{(K_m)^2}{V} \quad (6)$$

where K_m is the machine constant in $[\text{Nm}/\text{A}/\text{W}^{-(1/2)}]$, V is the volume of the machine $[\text{m}^3]$. The machine constant can be further expressed as in Eq. (7).

$$K_m = \frac{K_T}{\sqrt{P}} Z \quad (7)$$

where K_T is the torque constant $[\text{Nm}/\text{A}]$ and P is the input power to the coil winding $[\text{W}]$. The torque constant is given as in Eq. (8).

$$K_T = \frac{T_{avg}}{I} \quad (8)$$

where T_{avg} is the fundamental torque $[\text{Nm}]$ and I is the maximum current input to the machine $[\text{A}]$.

The comparative evaluation between typical double rotor switched reluctance machine, and improved double rotor switched reluctance machine in the same size is shown in the Table 2. It is clearly seen IDRSRM shows a better average torque density and higher motor constant square density compared to DRSRM.

Table. 2. Comparative evaluations.

Figure of Merit	DRSRM	IDRSRM
I [A]	7	7
V [m³]	1.99e ⁻³	2.11e ⁻³
T_{avg} [Nm]	0.7243	1.1584
K_t [Nm/A]	0.1035	0.1655
K_m [Nm/A/W^{($\frac{1}{2}$)]}	0.0104	0.0166
G [Nm²/A²/W/m³]	0.0544	0.1306

The comparative evaluation on ripple torque of the switched reluctance machines model in the same size is presented in Table 3 below.

Table. 3. Comparison on ripple torque.

Figure of Merit	DRSRM	IDRSRM
T_{avg} [Nm]	0.7243	1.1584
T_{max} [Nm]	3.3504	1.9127
T_{min} [Nm]	-0.0223	-2.44e ⁻⁵
T_r [%]	465.65	165.12

The improved DRSRM has the lowest ripple torque in comparison conventional double rotor switched reluctance machine which obviously shows a promising direction in reluctance machine research.

5. Conclusions

The improved double rotor switched reluctance machine is designed based on the double rotor structure and circular hole in the stator pole structure. There is a huge improvement of the improved double rotor switched reluctance machine. The motor constant square density is increased by 140% and the torque ripple is reduced by 64.5% compared to double rotor switched reluctance machine.

References

1. Aravind, C.V.; Norhisam, M.; Aris, I.; Ahmad, D.; and Nirei, M. (2011). Double rotor switched reluctance motors: fundamentals and magnetic circuit analysis. *IEEE Student Conference on Research and Development (SCORED2011) Kuala Lumpur*, 294-299.
2. Chockalingam, A.V.; Norhisam, M.; Mohammad, R.Z.; Ishak, A.; and Mohammad, H.M. (2012). Computation of electromagnetic torque in a double rotor switched reluctance motor using flux tube methods. *Energies*, 5(10), 4008-4026.

3. Norhisam, M.; Ridzuan, S.; Firdaus, R.N.; Aravind, C.V.; Wakiwaka, H.; and Nirei, N. (2012). Comparative evaluation on power speed density of portable permanent magnet generators for agricultural application. *Progress in Electromagnetics Research*, 129(1), 345-363.
4. Aravind, C.V.; Tay, S.C.; Jagadeeswaran, A; and Firdaus, R.N. (2014). Design of MAGLEV-VAWT with modified magnetic circuit generator. *Second International Conference on Electrical Energy Systems, India*.
5. Chockalingam, A.V.; Norhisam, M.; Ishak, A.; Mohammad, H.M.; and Masami, Nirei. (2013). Electromagnetic design and FEM analysis of a novel dual air-gap reluctance machine. *Progress in Electromagnetics Research*, 140(1), 523-544.
6. Mikail, R.; Husain, I; Sozer, Y.; Islam, M.; and Sebastian, T. (2012). Four-quadrant torque ripples minimization of switched reluctance machine through current profiling with mitigation of rotor eccentricity problem and sensor errors. *IEEE Energy Conversion Congress and Exposition*, 838-842.
7. Aravind, C.V.; Norhisam, M.H.; and Aris, I. (2012). Analytical design of double rotor switched reluctance motor using optimal pole arc values. *International Review in Electrical and Electronics*, 7(1), 3314-3324.
8. Mikail, R.; Sozer, Y.; Husain, I; Islam, M.; and Sebastian, T. (2011). Torque ripple minimization of switched reluctance machines through current profiling. *IEEE Energy Conversion Congress and Exposition*, 3568-3574.
9. Grace, I; Teymourzadeh, R.; Bright, S.; and Aravind, C.V. (2011). Optimised toolbox for the design of rotary reluctance motors. *IEEE International Conference on Sustainable Utilization and Development in Engineering and Technology*, 1-6.
10. Aravind, C.V.; Grace, I; Rozita, T.; Rajparthiban, R.; Rajprasad, R.; and Wong, Y.V. (2012). Universal computer aided design for electrical machines. , *8th International IEEE Colloquium on Signal Processing and its Applications*, 99-104.
11. Reynold, H. (2014). *Improvement in torque density of the double rotor switched reluctance machine*. Bachelor Thesis, Taylor's University, Selangor, Malaysia.
12. Aravind, C.V. (2013). *Design and implementation of double rotor switched reluctance motor using flux tube methods*. PhD thesis, University Putra Malaysia, Selangor, Malaysia.
13. Faiz, J. (2012). Performance improvement of a switched reluctance motor. *Progress In Electromagnetics Research Symposium (PIERS) Proceedings*, 728-732.